New Journal of Physics

The open access journal at the forefront of physics

PAPER

Frustrated double ionization of atoms in circularly polarized laser fields

HuiPeng Kang[1,2,3]* , Shi Chen[4,5] , Jing Chen[6,7] and Gerhard G Paulus[1,2]

1   Institute of Optics and Quantum Electronics, Friedrich Schiller University Jena, Max-Wien-Platz 1, 07743 Jena, Germany
2   Helmholtz Institut Jena, Frötbelstieg 3, 07743 Jena, Germany
3   State Key Laboratory of Magnetic Resonance and Atomic and Molecular Physics, Wuhan Institute of Physics and Mathematics, Innovation Academy for Precision Measurement Science and Technology, Chinese Academy of Sciences, Wuhan 430071, People's Republic of China
4   School of Physics, Peking University, Beijing 100871, People's Republic of China
5   HEDPS, Center for Applied Physics and Technology, Peking University, Beijing 100871, People's Republic of China
6   Institute of Applied Physics and Computational Mathematics, P.O. Box 8009, Beijing 100088, People's Republic of China
7   Center for Advanced Material Diagnostic Technology, College of Engineering Physics, Shenzhen Technology University, Shenzhen 518118, People's Republic of China
*   Author to whom any correspondence should be addressed.

E-mail: H.Kang@hi-jena.gsi.de

Abstract

We theoretically study frustrated double ionization (FDI) of atoms subjected to intense circularly polarized laser pulses using a three-dimensional classical model. We find a 'knee' structure of FDI probability as a function of intensity, which is similar to the intensity dependence of nonsequential double ionization probability. The observation of FDI is more favourable when using targets with low ionization potentials and short driving laser wavelengths. This is attributed to the crucial role of recollision therein, which can be experimentally inferred from the photoelectron momentum distribution generated by FDI. This work provides novel physical insights into FDI dynamics with circular polarization.

1. Introduction

When interacting with an intense laser pulse, the electrons in atoms or molecules can be strongly driven by the laser field, leading to various highly nonlinear phenomena mostly accompanied by photoionization. Interestingly, even for such strong laser field a substantial portion of electrons can be trapped into high-lying Rydberg states rather than being released into the continuum [1]. Rydberg state excitation of atoms and molecules has a wide range of applications in acceleration of neutral particles [2], precision measurements [3], generation of near-threshold harmonics [4], and quantum information [5]. In the past few years there is a growing interest in understanding the mechanism of Rydberg state excitation in strong laser fields [6–10].

The formation of excited Rydberg states has been experimentally identified for rare gas atoms, which is dubbed frustrated tunneling ionization [1]. Subsequently it was shown that during molecular double ionization (DI), one of the two emitted electrons may be trapped by the fragments generated by Coulomb explosion of molecules, giving rise to the formation of highly excited neutral fragments and singly charged ion fragments [11]. This process can be coined as frustrated double ionization (FDI). FDI has been the focus of intense studies for various molecular systems such as H_2 [11, 12], D_2 [13, 14], O_2 [15], N_2 [16], CO [17], and clusters [18–21]. In particular, theoretical studies using semiclassical model have been performed to identify different pathways leading to molecular FDI [22–25]. Recently, it has also been shown that FDI yields can be enhanced by adjusting the parameters of two-color counter-rotating circular fields [26]. However, FDI of atoms has attracted much less attention. From experimental point of view, molecular FDI can be identified by measuring the kinetic energy release during Coulomb explosion of molecules, which can not be applied to atomic targets without dissociation. Very recently, Larimian *et al*

reported coincident measurements on FDI of Ar atoms [27]. It was found that atomic FDI shows a strong dependence on laser intensity. For high intensities where sequential double ionization (SDI) dominates, electron trapping mainly happens during the second ionization step. For modest intensities where nonsequential (recollision-induced) double ionization (NSDI) dominates, the electron momentum distributions produced by FDI show features similar to that from DI. Detailed theoretical studies have shown that recollision and ionization-exit velocity distribution play important roles in atomic FDI [28–30].

Most of the investigations of FDI mentioned above adopted linearly polarized light. It is well known that in the case of elliptical or circular polarization, the additional transverse electric field of the laser light steers away the recolliding electrons and thus reduces the chance of recollision. Therefore, NSDI yields are expected to be decreased rapidly as the light ellipticity is increased, which has been verified for rare gases [31]. However, significant NSDI contributions have been observed for Mg atoms and small molecules with circularly polarized light [32, 33]. Theoretical studies employing semiclassical and fully classical models have shown that efficient recollision-induced DI with circular polarization is still possible via specific trajectories [34–37]. On the other side, whether FDI exists and how to understand its dynamics in (single-color) circularly polarized laser fields remains an open question.

In this paper we numerically study FDI of atoms with circularly polarized light using a three-dimensional classical ensemble method. Our calculations reveal significant contributions of FDI and we show that its observation is more favourable for the targets with low ionization potentials and short laser wavelengths. We find that for high intensities where SDI dominates, the first ionized electron is more likely to be captured after the end of the laser pulse, which is in contrast with the case by linear polarization. For intensities corresponding to the NSDI regime, the FDI probability as a function of intensity exhibits a 'knee' structure. Furthermore, recollision plays an important role in FDI for all the intensities studied here. This can be experimentally verified by measuring the photoelectron momentum distribution from FDI.
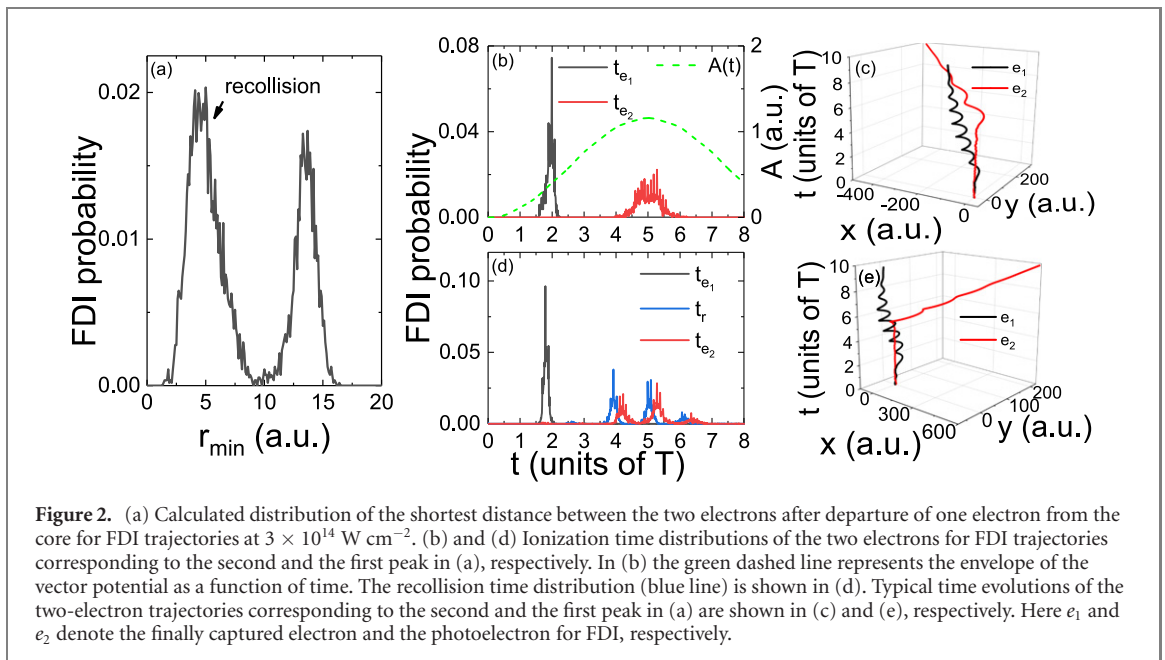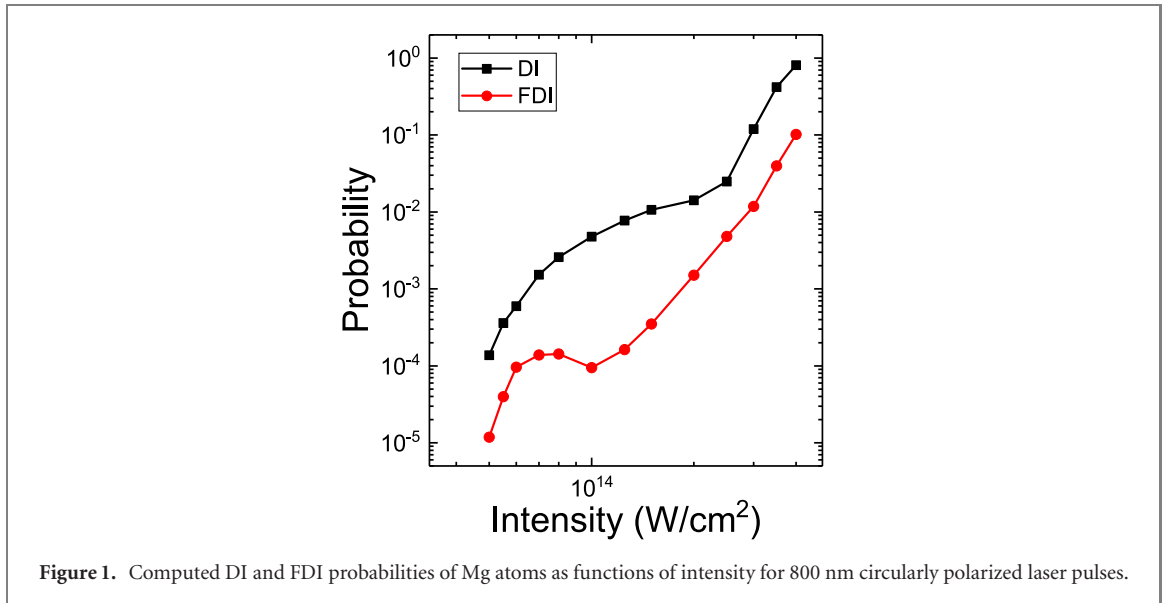
2. Theoretical model

Currently accurate quantum simulations of a two-active-electron system in a strong laser field still present a great challenge. Here we employ the well-established classical model developed by Eberly and co-workers [38] to study FDI of atoms with circularly polarized light. This model has shown remarkable success in explaining many important features of strong-field DI [39–45]. Within this model, the evolution of a two-active-electron atom is described by the classical Newtonian equation of motion (atomic units are used throughout this paper):

$$\frac{\mathrm{d}^2 \mathbf{r_i}}{\mathrm{d}t^2} = -\mathbf{E}(t) - \nabla(V_{\mathrm{ne}}^i + V_{\mathrm{ee}}), \tag{1}$$

where $\mathbf{E}(t) = (E_x(t), E_y(t), 0)$ is the circularly polarized laser field with $E_x(t) = E_0/\sqrt{2}f(t)\cos\omega t$ and $E_y(t) = E_0/\sqrt{2}f(t)\sin\omega t$ (ω is the laser frequency). Here E_0 is the peak amplitude of the laser electric field and $f(t) = \sin^2[\pi t/(10T)]$ is the pulse envelope function with the full duration of $10T$, where T is the optical cycle. The index $i = 1, 2$ in equation (1) denote the two active electrons. The Coulomb interaction potential between the nucleus and the ith electron is $V_{\mathrm{ne}}^i = -2/\sqrt{\mathbf{r}_i^2 + a^2}$ and $V_{\mathrm{ee}} = 1/\sqrt{(\mathbf{r}_1 - \mathbf{r}_2)^2 + b^2}$ represents the potential for the electron–electron interaction. The softening parameters a and b are introduced to avoid autoionization and numerical singularity [46, 47]. The values of a and b are set to be 3.0 a.u. and 0.05 a.u. for Mg atoms [44]. For Ar atoms, we choose $a = 1.5$ a.u. and $b = 0.05$ a.u. [29].

The initial conditions of the two electrons are obtained by first randomly assigning their positions in the classical allowed region for the energy corresponding to the negative sum of the first and second ionization potentials of the target atom. The remaining energy is randomly distributed between the two electrons in momentum space. To obtain stable position and momentum distributions, the system is allowed to evolve without the laser field for a sufficiently long time (about 100 a.u.). The laser field is switched on once the initial ensemble is stable. The evolution of the two-electron system is traced until the end of the laser pulse according to the Newtonian equation. The energy of each electron contains potential energy of the electron–ion interaction, the kinetic energy, and half of the electron–electron repulsion energy. A double-ionization event is identified when the final energies of both electrons are greater than zero. For FDI events, the two electrons achieve positive energies during the laser pulse [29, 30]. At the end of the laser pulse, one electron has positive final energy but the other is captured and has negative final energy above $-I_{p2}$, where I_{p2} is the second ionization potential of the target atom.

Figure 1. Computed DI and FDI probabilities of Mg atoms as functions of intensity for 800 nm circularly polarized laser pulses.

Figure 2. (a) Calculated distribution of the shortest distance between the two electrons after departure of one electron from the core for FDI trajectories at 3×10^{14} W cm^{-2}. (b) and (d) Ionization time distributions of the two electrons for FDI trajectories corresponding to the second and the first peak in (a), respectively. In (b) the green dashed line represents the envelope of the vector potential as a function of time. The recollision time distribution (blue line) is shown in (d). Typical time evolutions of the two-electron trajectories corresponding to the second and the first peak in (a) are shown in (c) and (e), respectively. Here e_1 and e_2 denote the finally captured electron and the photoelectron for FDI, respectively.

3. Numerical results and discussions

Figure 1 shows the calculated probabilities of DI and FDI for Mg as functions of intensity. The characteristic 'knee' structure indicating NSDI contributions below $\sim 2 \times 10^{14}$ W cm^{-2} can be clearly seen in DI results. Above this intensity, SDI starts to dominate. This is in good agreement with previous experiments [32] and theoretical simulations [34–36]. Our calculations also reveal the existence of significant FDI contributions by circular polarization. Interestingly, a similar 'knee' shape below 1×10^{14} W cm^{-2} is also found in FDI results. Below we explore in detail the physical mechanism of FDI, which is the main focus of our paper.

Our discussions start with the intensities where SDI dominates. In figure 2(a) we show the distribution of the closest distance between the two electrons after the emission of one electron from the core for FDI events at 3×10^{14} W cm^{-2}. The ionization exit of the first emitted electron ranges from 12 a.u. to 17 a.u. Here the ionization exit indicates the distance when the ionized electron obtains a total positive energy for the first time. The first peak below 10 a.u. indicates that recollision occurs. This means that, surprisingly, for SDI regime where recollision plays a minor role, more than half FDI events are still connected to recollision.

To understand FDI dynamics, we first calculate ionization time distributions of the two electrons for the FDI events that are not related to recollision. Here the ionization time is defined when the energy of the electron becomes positive for the first time [29]. Within our model, the two electrons can be distinguished
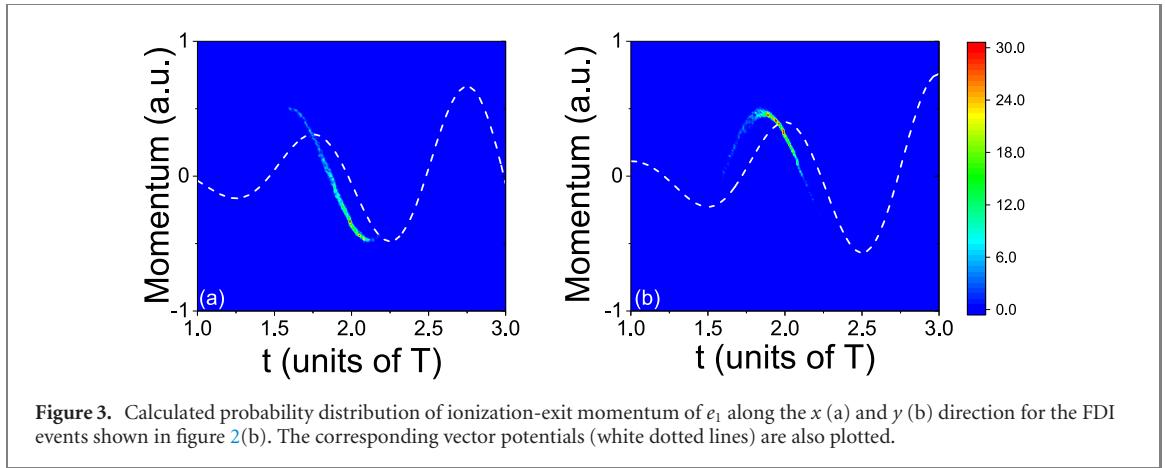
Figure 3. Calculated probability distribution of ionization-exit momentum of e_1 along the x (a) and y (b) direction for the FDI events shown in figure 2(b). The corresponding vector potentials (white dotted lines) are also plotted.
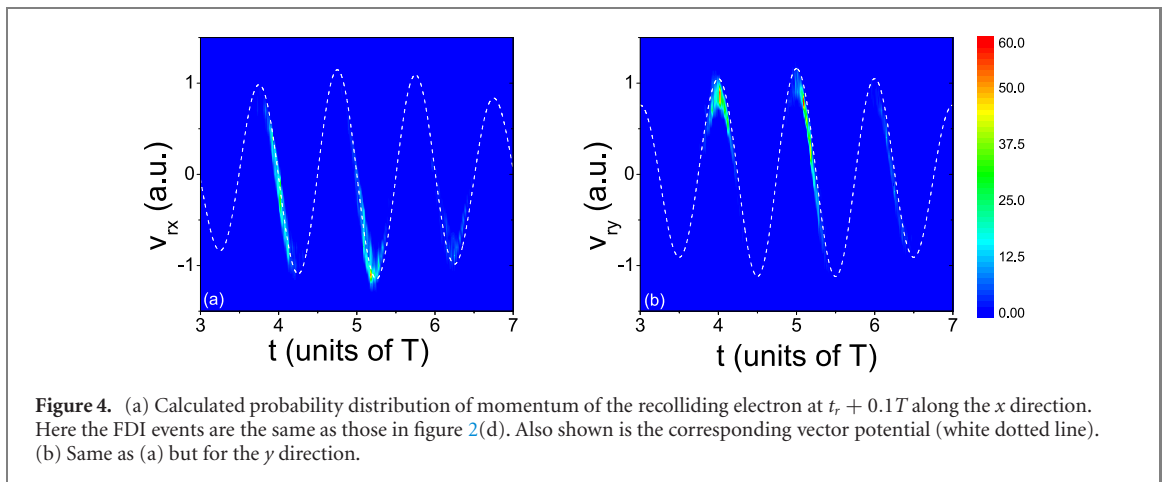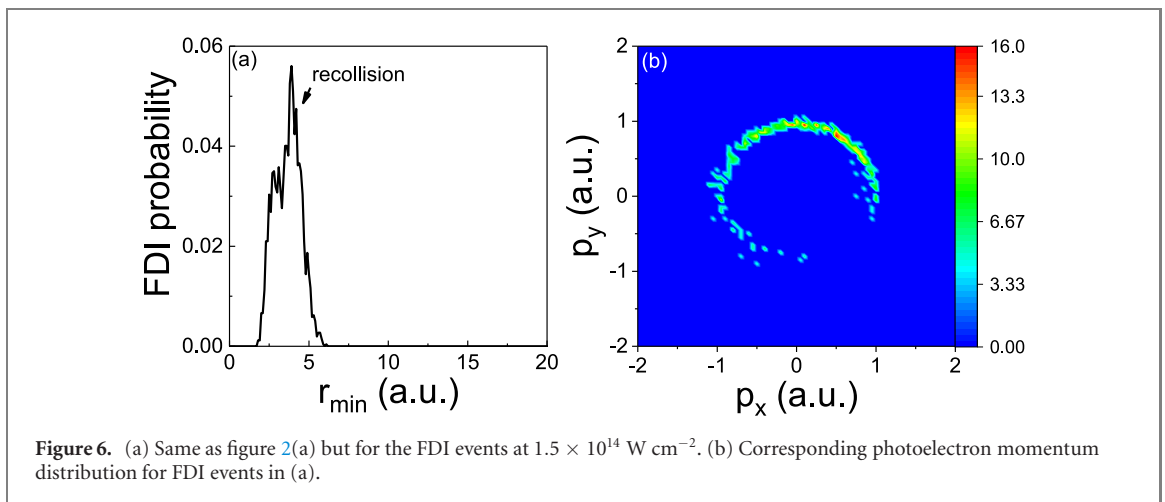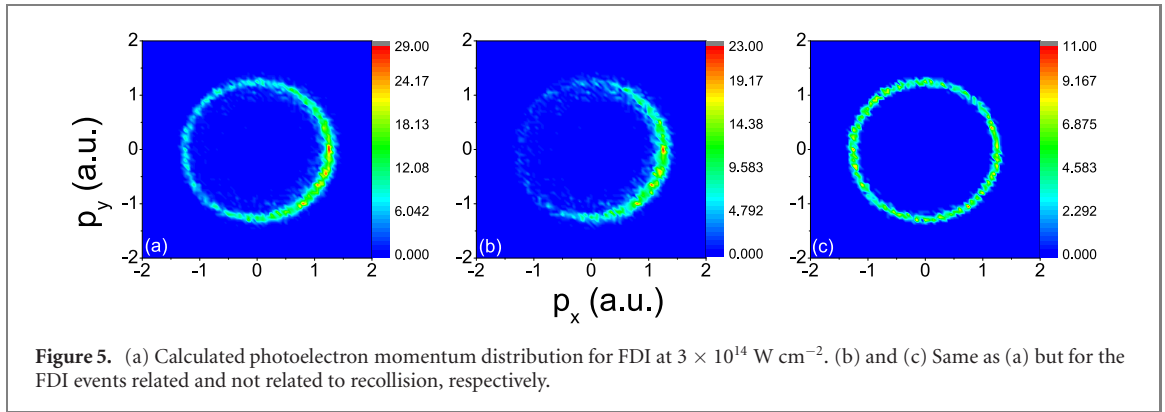

Figure 4. (a) Calculated probability distribution of momentum of the recolliding electron at $t_r + 0.1T$ along the x direction. Here the FDI events are the same as those in figure 2(d). Also shown is the corresponding vector potential (white dotted line). (b) Same as (a) but for the y direction.

according to which one is captured at the end of the laser pulse. These two electrons are ionized independently and one cannot expect strong correlations between them. As seen in figure 2(b), the finally captured electron e_1 is ionized during the rising edge of the laser envelope, while the other electron e_2 (the photoelectron generated by FDI) is ionized around the peak of the laser envelope. This can be easily understood as the electron ionized around the peak obtains much larger drift momentum $-A(t_{e_2})$ from the laser field, making it more difficult to be captured at the end of the laser pulse. The calculations also demonstrate that for SDI regime, the early ionized electron tends to be captured, which is in striking contrast to the case by linearly polarized laser fields [27]. A typical two-electron trajectory is displayed in figure 2(c). We find that the ionization-exit momentum of e_1 is not completely compensated by the drift momentum $-A(t_{e_1})$ obtained from the laser field (figure 3), revealing the important role of Coulomb focusing effects in FDI.

For the FDI events related to recollision, the dynamics is different. The finally captured electron is ionized during the rising edge and returns to the core several times around the peak of the laser envelope [figure 2(d)]. The calculated distribution of recollision time t_r is shown in figure 2(d). Here the recollision time is defined as the instant of closest approach of the two electrons after departure of one electron from the core [40]. During recollision, a small portion of the energy of the returning electron is transferred to the second electron, which is ionized shortly after recollision and contributes to the photoelectron for FDI. In the polarization plane (x–y plane), right after recollision both the residual momenta of the returning electron along the x and y axis, i.e. v_{rx} and v_{ry}, are largely compensated by the drift momenta obtained from the laser field subsequently. This can be clearly seen in figure 4 where we show the calculated probability distributions of momenta of the returning electron at $t_r + 0.1T$ and the corresponding vector potentials. Neglecting Coulomb potential, both the final velocities along the x and y directions $p_{x,y} \approx v_{rx,ry} - A_{x,y}(t_r + 0.1T)$ are close to zero. Thus the rescattered electron tends to be captured after the end of the laser pulse. A typical two-electron trajectory showing such dynamics is depicted in figure 2(e).
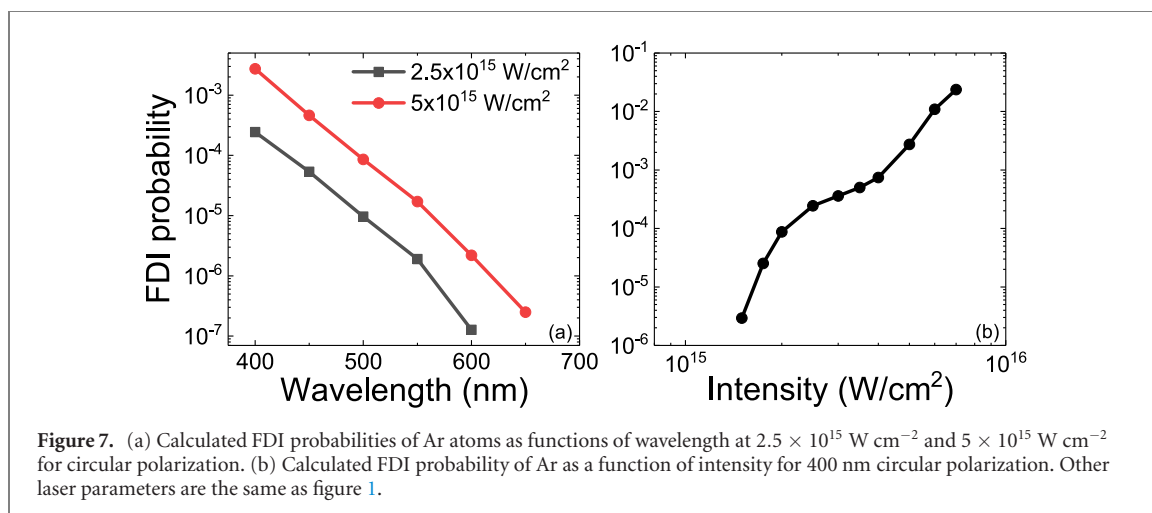
Next we show whether FDI is related to recollision can be inferred from the final momentum distribution of the photoelectrons produced by FDI, which can be measured using a reaction microscope. Figure 5(a) shows the calculated photoelectron momentum distribution for FDI at 3×10^{14} W cm^{-2}. One

Figure 5. (a) Calculated photoelectron momentum distribution for FDI at 3×10^{14} W cm^{-2}. (b) and (c) Same as (a) but for the FDI events related and not related to recollision, respectively.

Figure 6. (a) Same as figure 2(a) but for the FDI events at 1.5×10^{14} W cm^{-2}. (b) Corresponding photoelectron momentum distribution for FDI events in (a).

can find a doughnut-like structure with more electron yield in a crescent-shaped distribution. This is different from the electron momentum distribution from single ionization by circular polarization, which exhibits a symmetric doughnut-like shape [48]. In figures 5(b) and (c) we show the electron momentum distributions for the FDI events related and not related to recollision, respectively. The comparison between figures 5(b) and (c) reveals that the asymmetric electron yields in figure 5(a) arise from recollision, which occurs every cycle mainly within the range from $3.5T$ to $5.5T$ [see figure 2(d)]. The ionization time distribution of the photoelectron shows similar features and each peak covers a half laser cycle [see figure 2(d)]. Therefore, the photoelectron obtains drift momentum from the laser field every half cycle, resulting in the crescent-shaped distribution shown in figure 5(b). For FDI trajectories not related to recollision, the ionization time distribution of the photoelectron almost covers one laser cycle [figure 2(b)], leading to the symmetric doughnut-like shape shown in figure 5(c).

For modest intensities where NSDI dominates, the mechanism of FDI is similar to that of the FDI events related to recollision at 3×10^{14} W cm^{-2}. In figure 6(a) we show the calculated distribution of the closet approach of the two electrons after the ionization of one electron for FDI events at 1.5×10^{14} W cm^{-2}. The calculation shows a single peak below 10 a.u., indicating that all FDI events are related to recollision. The ionization of the photoelectron is closely connected to the recollision, which occurs every cycle around the peak of the laser envelope (not shown). As explained above, this leads to the crescent-shaped distribution of the photoelectron momentum shown in figure 6(b). Again, the calculations indicate that recollision leaves its footprints in the photoelectron momentum distribution, which can be experimentally verified. Note that, to observe the crescent structure shown in figures 5 and 6, the carrier-envelope phase of the laser pulses has to be stabilized.

It is well known that the 'knee' structure of DI probability as a function of intensity is a consequence of recollision. Furthermore, it has been shown that recollision is universal in circularly polarized laser fields [49] and to observe this 'knee' structure, the laser frequency has to be larger than $0.18(I_{p1})^{5/4}$, where I_{p1} is the first ionization potential of the target [36]. Therefore, the observation of the 'knee' shape by circular polarization favours targets with low ionization potentials such as Mg and short driving laser wavelengths. This is why the 'knee' structure has escaped observation for DI of rare gas atoms with circular polarization at 800 nm. For FDI, we have demonstrated the crucial role of recollision for the whole range of intensities

Figure 7. (a) Calculated FDI probabilities of Ar atoms as functions of wavelength at 2.5×10^{15} W cm^{-2} and 5×10^{15} W cm^{-2} for circular polarization. (b) Calculated FDI probability of Ar as a function of intensity for 400 nm circular polarization. Other laser parameters are the same as figure 1.

covering both NSDI and SDI regimes. Consequently, one can expect that FDI probability will be significantly decreased for atoms with high ionization potentials and for long wavelengths where recollision is suppressed. In figure 7(a) we show the calculated FDI probabilities of Ar atoms as functions of wavelength for two different intensities. Indeed, the FDI probability decreases rapidly as the wavelength is increased. For wavelengths longer than 650 nm, the FDI probability is too small to be calculated, which is in accordance with the absence of NSDI of Ar for such wavelengths [36, 49]. Figure 7(b) shows the FDI probability of Ar as a function of intensity for 400 nm circularly polarized laser fields. One can see a 'knee' structure similar to the FDI calculation for Mg at 800 nm. This is in line with the prediction for DI that recollision is more favourable for rare gases with short wavelengths [49].

4. Conclusion

In conclusion, we have theoretically investigated FDI of atoms exposed to intense circularly polarized laser pulses. The simulations revealed a 'knee' structure of FDI probability as a function of intensity, which is similar to DI results at modest intensities. We demonstrated that, to observe FDI with circular polarization, it is beneficial to employ targets with low ionization potentials and short laser wavelengths. This is due to the fact that recollision plays an essential role in FDI not only for the NSDI regime but also for the SDI regime. We further showed that recollision can be experimentally identified from the photoelectron momentum distribution produced by FDI.
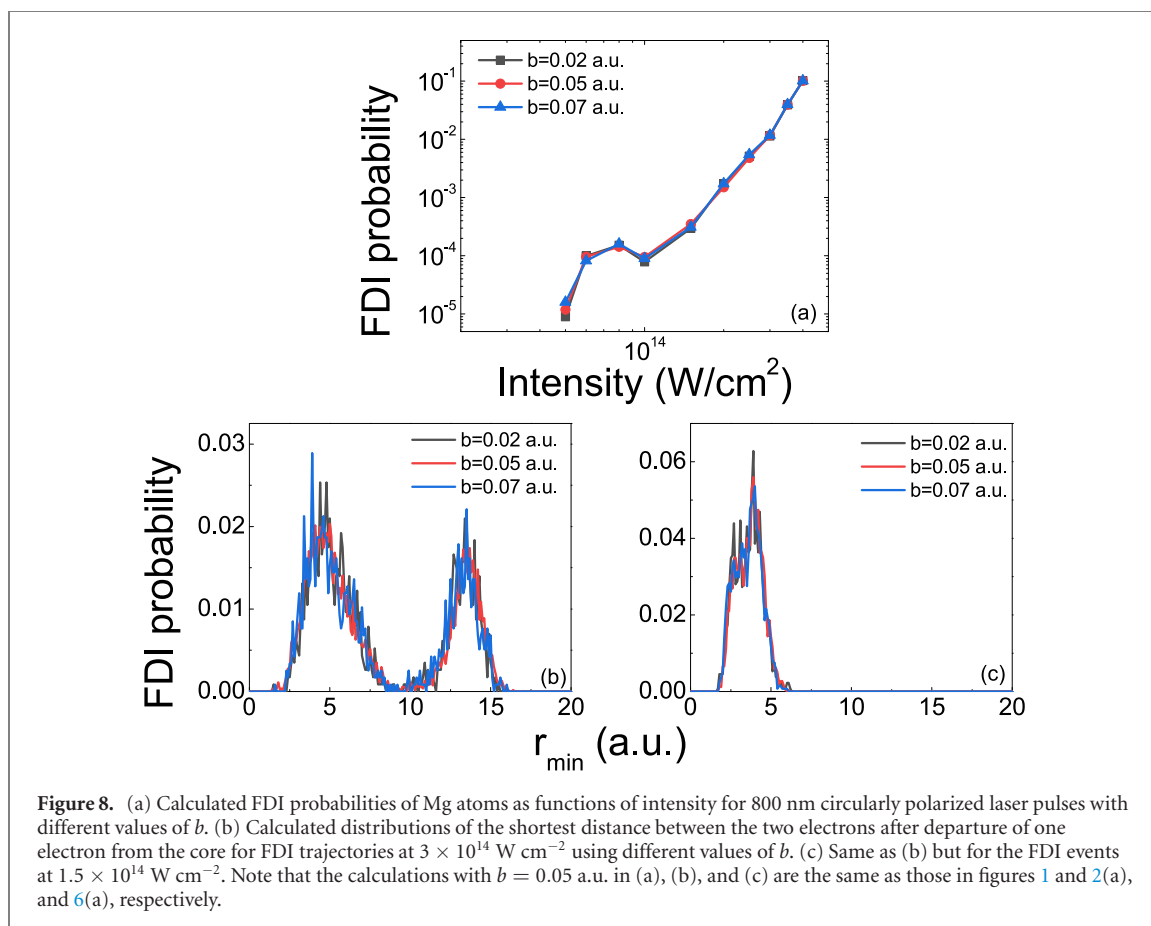
Data availability statement

The data that support the findings of this study are available upon reasonable request from the authors.

Appendix.

The softening parameter *a* in the electron–nucleus potential in equation (1) is introduced to avoid auto-ionization. In our simulations for Mg, we choose $a = 3.0$ a.u. in order to keep the initial conditions of the electrons stable. In addition, as well justified in previous studies (see, e.g. [35, 43]), using this value, the calculated DI curve agrees well with the experimental result. The other softening parameter *b* for the electron–electron interaction is used to avoid mathematical singularity in the calculations. The simulated results will not be changed once this value is sufficiently small. To check whether our calculated results

Figure 8. (a) Calculated FDI probabilities of Mg atoms as functions of intensity for 800 nm circularly polarized laser pulses with different values of *b*. (b) Calculated distributions of the shortest distance between the two electrons after departure of one electron from the core for FDI trajectories at 3×10^{14} W cm^{-2} using different values of *b*. (c) Same as (b) but for the FDI events at 1.5×10^{14} W cm^{-2}. Note that the calculations with $b = 0.05$ a.u. in (a), (b), and (c) are the same as those in figures 1 and 2(a), and 6(a), respectively.

depend on *b*, we perform calculations with different values of *b*, as displayed in figure 8. Figure 8(a) shows the FDI probabilities of Mg atoms as a function of intensity for 800 nm circularly polarized laser pulses with different values of *b*. The FDI probabilities almost stay unchanged when *b* is varied. Figures 8(b) and (c) show the calculated distributions of $r_{\min}$ (the shortest distance between the two electrons after departure of one electron from the core) for FDI trajectories at 3×10^{14} W cm^{-2} and 1.5×10^{14} W cm^{-2}, respectively. The results show no obvious dependence on *b*. The situation is similar for the calculations of Ar. This indicates that our main findings and analysis do not depend on the exact value of *b*.

ORCID iDs

HuiPeng Kang ⓘ https://orcid.org/0000-0002-4255-0778
Shi Chen ⓘ https://orcid.org/0000-0001-7864-4496

References

[1]   Nubbemeyer T, Gorling K, Saenz A, Eichmann U and Sandner W 2008 *Phys. Rev. Lett.* **101** 233001
[2]   Eichmann U, Nubbemeyer T, Rottke H and Sandner W 2009 *Nature* **461** 1261
[3]   Facon A, Dietsche E-K, Grosso D, Haroche S, Raimond J-M, Brune M and Gleyzes S 2016 *Nature* **535** 262
[4]   Xiong W H, Geng J W, Tang J Y, Peng L Y and Gong Q 2014 *Phys. Rev. Lett.* **112** 233001
[5]   Saffman M, Walker T G and Mølmer K 2010 *Rev. Mod. Phys.* **82** 2313
[6]   von Veltheim A, Manschwetus B, Quan W, Borchers B, Steinmeyer G, Rottke H and Sandner W 2013 *Phys. Rev. Lett.* **110** 023001
[7]   Huang K Y, Xia Q Z and Fu L B 2013 *Phys. Rev. A* **87** 033415
[8]   Li Q, Tong X M, Morishita T, Wei H and Lin C D 2014 *Phys. Rev. A* **89** 023421
[9]   Popruzhenko S V 2017 *J. Phys. B: At. Mol. Opt. Phys.* **51** 014002
[10] Zimmermann H, Buller J, Eilzer S and Eichmann U 2015 *Phys. Rev. Lett.* **114** 123003
[11] Manschwetus B, Nubbemeyer T, Gorling K, Steinmeyer G, Eichmann U, Rottke H and Sandner W 2009 *Phys. Rev. Lett.* **102** 113002
[12] Zhang W *et al* 2017 *Phys. Rev. Lett.* **119** 253202
[13] McKenna J *et al* 2011 *Phys. Rev. A* **84** 043425
[14] Zhang W *et al* 2018 *Phys. Rev. A* **98** 013419
[15] Ma J *et al* 2019 *Phys. Rev. A* **100** 063413
[16] Nubbemeyer T, Eichmann U and Sandner W 2009 *J. Phys. B: At. Mol. Opt. Phys.* **42** 134010
[17] Zhang W *et al* 2020 *Phys. Rev. A* **101** 033401

[18] Ulrich B, Vredenborg A, Malakzadeh A, Meckel M, Cole K, Smolarski M, Chang Z, Jahnke T and Dörner R 2010 *Phys. Rev. A* **82** 013412

[19] Manschwetus B, Rottke H, Steinmeyer G, Foucar L, Czasch A, Schmidt-Böcking H and Sandner W 2010 *Phys. Rev. A* **82** 013413

[20] Wu J *et al* 2011 *Phys. Rev. Lett.* **107** 043003

[21] Xie X, Wu C, Liu H, Li M, Deng Y, Liu Y, Gong Q and Wu C 2013 *Phys. Rev. A* **88** 065401

[22] Emmanouilidou A, Lazarou C, Staudte A and Eichmann U 2012 *Phys. Rev. A* **85** 011402

[23] Price H, Lazarou C and Emmanouilidou A 2014 *Phys. Rev. A* **90** 053419

[24] Chen A, Price H, Staudte A and Emmanouilidou A 2016 *Phys. Rev. A* **94** 043408

[25] Chen A, Kling M F and Emmanouilidou A 2017 *Phys. Rev. A* **96** 033404

[26] Katsoulis G P, Sarkar R and Emmanouilidou A 2020 *Phys. Rev. A* **101** 033403

[27] Larimian S, Erattupuzha S, Baltuška A, Kitzler-Zeiler M and Xie X 2020 *Phys. Rev. Res.* **2** 013021

[28] Shomsky K N, Smith Z S and Haan S L 2009 *Phys. Rev. A* **79** 061402

[29] Li Y, Xu J, Yu B and Wang X 2020 *Opt. Express* **28** 7341

[30] Chen S, Chen J, Paulus G G and Kang H 2020 *Phys. Rev. A* **102** 023103

[31] Dietrich P, Burnett N H, Ivanov M and Corkum P B 1994 *Phys. Rev. A* **50** R3585

[32] Gillen G D, Walker M A and Van Woerkom L D 2001 *Phys. Rev. A* **64** 043413

[33] Cornaggia C and Hering P 2000 *Phys. Rev. A* **62** 023403

[34] Wang X and Eberly J H 2010 *Phys. Rev. Lett.* **105** 083001

[35] Mauger F, Chandre C and Uzer T 2010 *Phys. Rev. Lett.* **105** 083002

[36] Fu L B, Xin G G, Ye D F and Liu J 2012 *Phys. Rev. Lett.* **108** 103601

[37] Kamor A, Mauger F, Chandre C and Uzer T 2013 *Phys. Rev. Lett.* **110** 253002

[38] Panfili R, Eberly J H and Haan S L 2001 *Opt. Express* **8** 431

[39] Ho P J, Panfili R, Haan S L and Eberly J H 2005 *Phys. Rev. Lett.* **94** 093002

[40] Haan S L, Van Dyke J S and Smith Z S 2008 *Phys. Rev. Lett.* **101** 113001

[41] Mauger F, Chandre C and Uzer T 2009 *Phys. Rev. Lett.* **102** 173002

[42] Wang X, Tian J and Eberly J H 2013 *Phys. Rev. Lett.* **110** 073001

[43] Xu T T, Ben S, Wang T, Zhang J, Guo J and Liu X S 2015 *Phys. Rev. A* **92** 033405

[44] Ben S, Guo P-Y, Song K-L, Xu T-T, Yu W-W and Liu X-S 2017 *Opt. Express* **25** 1288

[45] Chen Y, Zhou Y, Li Y, Li M, Lan P and Lu P 2016 *J. Chem. Phys.* **144** 024304

[46] Javanainen J, Eberly J H and Su Q 1988 *Phys. Rev. A* **38** 3430

[47] Su Q and Eberly J H 1991 *Phys. Rev. A* **44** 5997

[48] Alnaser A S, Tong X M, Osipov T, Voss S, Maharjan C M, Shan B, Chang Z and Cocke C L 2004 *Phys. Rev. A* **70** 023413

[49] Chen X, Wu Y and Zhang J 2017 *Phys. Rev. A* **95** 013402